THE JOURNAL OF PHYSICAL CHEMISTRY C

ARTICLE

pubs.acs.org/JPCC

Effect of Compensated Codoping on the Photoelectrochemical Properties of Anatase TiO_2 Photocatalyst

Xinguo Ma,[†] Ying Wu,[‡] Yanhui Lu,[†] Jing Xu,[†] Yajun Wang,[†] and Yongfa Zhu*[,†]

[†]Department of Chemistry, Tsinghua University, Beijing 100084, People's Republic of China

[‡]Department of Electronic Science and Technology, Huazhong University of Science and Technology, Wuhan 430074, People's Republic of China

ABSTRACT: An effective codoping approach is described to modify the photoelectrochemical properties of anatase TiO_2 by doping with nonmetal (N or C) and transition metal (Nb or Ta) impurities. Here, compensated and noncompensated codoped TiO_2 systems are constructed with different proportions and dopant species, and then their dopant formation energies and electronic properties are calculated to study the stability and visible-light photoactivity by first-principles density functional theory incorporating the LDA+*U* formalism, respectively. The calculated results demonstrate that the codoping with transition metals facilitates the enhancement of the concentration of p-type dopants (N and C) in the host lattice. Especially, both 1:2 compensated Nb/C/Nb and Ta/C/Ta codopings not only reduce the energy gap to enhance the optical absorption and eliminate the local trapping to improve carrier mobility and conversion efficiency but also do not lower the reduction potential of the conduction band edge. Our designated strategies of codoped anatase TiO_2 simultaneously meet the criteria for water splitting. It should be pointed out that, to be successful, the proper proportion of transition metal and nonmetal impurities in the host lattice should be controlled so that reasonable photoelectrochemical properties can be achieved.

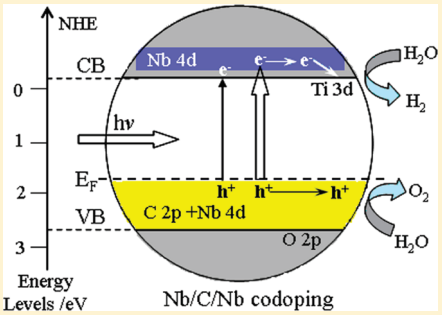

1. INTRODUCTION

TiO_2 has attracted extensive attention as a promising active semiconductor photocatalyst that degrades environmental pollutants[1,2] or directly splits water[3] under sunlight irradiation. However, as a wide band-gap semiconductor (e.g., 3.23 eV for anatase), TiO_2 can be only activated under ultraviolet-light irradiation, which accounts for a small proportion (less than 5%) of solar energy. It is desirable that the band gap of the semiconductor would be about 2.0 eV for the effective utilization of visible light. Therefore, great efforts were made to modify the band gap of TiO_2 by various methods,[4−12] but with only marginal success. The most common one used for band-gap reduction is the incorporation of impurities, such as N,[4−9] C,[10,11] B,[12] and so on. However, their incorporations also lead to poor photoresponse because the partially occupied impurity bands can act as killers for photogenerated carriers.[5] In addition, the p-type doping remains difficult due to its fairly lower valence band (VB) edges measured with respect to a fixed energy (e.g., vacuum level), which is similar to that of ZnO, InN, etc.[13,14]

Recently, codoped TiO_2 with nonmetals and transition metals (TMs) has become a rapidly growing field of interest and has met expectations both theoretically[15−17] and experimentally.[18−21] For example, the V/N-codoped TiO_2 photocatalyst synthesized by Gu et al.[18] shows the enhancement of photocatalytic activity for the degradation of methylene blue under visible-light irradiation (λ > 440 nm) compared with those of V-monodoped and N-monodoped TiO_2. Another example is that the Ni/B-codoped TiO_2 photocatalyst possesses superior photocatalytic activity to that of the as-prepared monodoped TiO_2 products.[21] These results indicate that codoped TiO_2 with nonmetals and TMs may be a new promising second-generation photocatalyst because donor−acceptor codoping may suppress the recombination and yet maintain a reduced energy gap.[15−19] The concepts of compensated (CP) and noncompensated (NCP) were established as the powerful guiding principle in the future designing of photocatalysts and other functional materials.[15,20] For the former, the electrons on the donor levels compensate the same amount of holes on the acceptor levels, so the systems still keep the semiconductor character. For the latter, the extra charge associated with the two dopants cannot be completely compensated by each other. Gai et al.[15] demonstrated a CP donor−acceptor codoping theory to explain the energy gap reduction and the suppression of recombination. On the contrary, Zhu et al.[20] proposed an NCP theory as an explanation for the photoresponse mechanism because of the higher carrier density. Those theories remain to be argued. In previous codoping investigations, V/N- and Cr/C-codoped TiO_2 show a narrowing of the band gap, but their impurity levels under the conduction band minimum (CBM) lower the reduction potential of the CB edge, resulting in poor water splitting.[15−17] As discussed above, the present achievements are still far from the ideal goal.

Received: March 24, 2011
Revised: June 22, 2011
Published: July 06, 2011

dx.doi.org/10.1021/jp202750w | *J. Phys. Chem. C* 2011, 115, 16963–16969

To design a "visible-light photocatalyst" using the codoping method for water splitting, one needs to identify impurities that (i) are soluble in the host to reduce the energy gap and enhance optical absorption, (ii) do not lower the conduction band minimum energy level, and (iii) are able to shed the photoexcited electrons transferring to the CBM of the host. Exhibiting high 4d and 5d atomic orbital energies, Nb and Ta are more likely to transfer their excess electrons to the CBM of the host than V having a much lower 3d atomic orbital energy.[22,23] In addition, N and C have higher atomic p orbital energies than O to form acceptor impurity levels above the VB maximum (VBM), which reduces a phototransition energy.[6,7,11] Therefore, Nb and Ta are predicted to be the best choices as donors, and N and C are the best choices as acceptors.

Up to now, there is no corresponding systemic theoretical report about the comparison of photoelectrochemical properties of CP and NCP codoped TiO_2. Thus, we specifically constructed CP and NCP codoping systems with different dopant pairs. Here, Nb/C- and Ta/C-codoped (1:1) TiO_2 are chosen as NCP models. Nb/N- and Ta/N-codoped (1:1) and Nb/C/Nb- and Ta/C/Ta-codoped (1:2) TiO_2 are chosen as CP models. In this work, we presented the calculated results of the formation energies and electronic properties of both CP and NCP codoping systems with different dopant pairs using first-principles density functional theory (DFT) incorporating the LDA+U formalism. Our strategies can overcome the difficulties of some previous schemes and may provide some guidance for improving the photoelectrochemical activity of anatase TiO_2 by the codoping approach.

2. METHODS

All of the spin-polarized DFT calculations were performed using a development version of the SIESTA code.[24] A double-ζ basis set with additional orbitals of polarization was employed. The Troullier−Martins scheme[25] was taken for the norm-conserving pseudopotentials. A grid cutoff of 150 Ry and a Monkhorst−Pack[26] k-points mesh of 5 × 5 × 5 were used for geometry optimization and electronic properties calculations. The doped systems were constructed from a relaxed 2 × 2 × 1 48-atom supercell of anatase TiO_2, with the atomic concentration of impurities comparable to experiments.[4,5,7,19,20] Standard local density approximation (LDA) and the generalized gradient approximation (GGA) functionals fail to give reasonably accurate results for their band characteristics and especially band-gap values, due to the self-interaction error inherent to such functionals.[27−29] The LDA+U approach aims to correct for this by adding an orbital-dependent term to the LDA potential. However, when the correction is only applied on transition metal d orbitals, the band-gap value is still underestimated compared to the experimental one, even at high U values.[30−32] Recently, a few theoretical studies on transition-metal oxides discussed the effect of the U parameter on the p electrons (U_p) of oxygen in addition to the d electrons (U_d) of the transition metal.[31−34]

A U(Ti d) value of 4.2 eV was applied to the Ti 3d orbitals in the present work. This value has been previously shown to provide a description of O vacancies at the TiO_2(110) surface that is in good agreement with the available spectroscopic data.[35−37] If the U is only incorporated for the Ti 3d states, the band-gap energies are increased with increasing U(Ti d) values from 0 to 15 eV, from a value of 2.15 eV within the conventional LDA to 3.17 eV within LDA+U_d; however, the band-gap energies are still underestimated compared to the experimental value of 3.23 eV (see inset of Figure 1). To determine U(O p), we used the fitting procedure of Lany and Zunger.[38] For the exact density functional, the energy change of the system is linear when part of the electrons are added or removed.[39] For addition of an electron to a hole state, this condition requires that

$$E(n_h + 1) - E(n_h) = e_i(n_h) \quad (1)$$

where $E(n_h + 1) - E(n_h)$ is the electron addition energy E_{ad}, that is, the difference in the energy between the system with a self-trapped hole present (the +1 charge state) and the neutral system, where both are calculated at the optimized geometry for the hole system, and $e_i(n_h)$ is the eigenvalue of the hole state relative to the VBM. Figure 1 shows the variation in E_{ad} and $e_i(n_h)$ for the +1 charge state of stoichiometric anatase TiO_2 with U(O p) (here, 4.2 eV is taken for U(Ti d)). It is obvious that eq 1 is satisfied for U(O p) = 4.02 eV, giving the correct splitting between occupied and unoccupied O 2p states. The result is smaller than U(O p) = 5.25 eV of ref 40 calculated using the projector augmented-wave method.

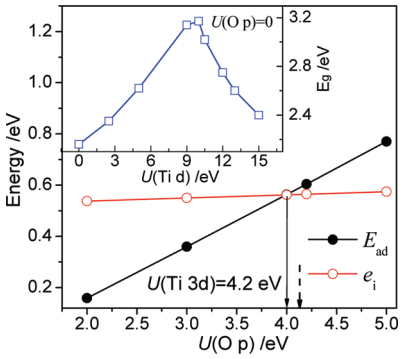

Figure 1. Electron addition energy, E_{ad}, and the eigenvalue $e_i(n_h)$ of the hole state of the +1 charge state of anatase TiO_2 as a function of the U(O p) parameter calculated within the LDA+U_d+U_p approach. The solid arrow shows the value of U(O p) for which eq 1 is satisfied. The U parameter corresponding to the experimental band gap is indicated by the dashed arrow. In addition, the band gap E_g as a function of the U(Ti d) parameter within the LDA+U_d approach is shown in the inset.

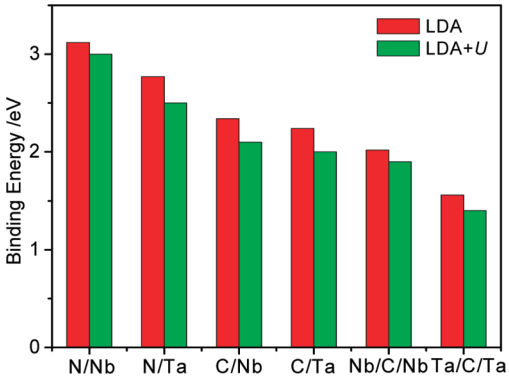

Figure 2. Calculated binding energies (in eV) of the X_{Ti}−Y_O complexes in TiO_2 with LDA (red) and LDA+U (green), where X = Nb, Ta and Y = N, C.

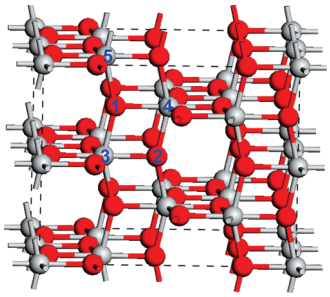

Figure 3. 2 × 2 × 1 supercell structure of anatase TiO_2. Gray and red spheres represent the Ti and O atoms, respectively. Roman numbers labeled on the O and Ti atoms are used to identify the doped configuration.

3. RESULTS AND DISCUSSION

3.1. Doped Configuration and Geometry Structure. The lattice parameters of a relaxed cell for pure anatase TiO_2 are found to be a = 3.789 Å and c = 9.550 Å within the spin-polarized LDA+U approach, in good agreement with experimental and other theoretical results.[41,42] The calculated Ti−O bond lengths are 1.954 and 1.997 Å, respectively. The doped systems are constructed from a relaxed 2 × 2 × 1 48-atom supercell of anatase TiO_2. Other theoretical results have identified that the Ti and O sites are preferentially substituted by the TMs and nonmetal atoms, respectively.[15−17,20] To see if the defect pairs can form, we calculated the binding energy of defect pairs in the host lattice. The binding energy E_b is defined as[15,43]

$$E_b = E_T(X_{Ti}) + E_T(Y_O) - E_T(X_{Ti} + Y_O) - E_T(TiO_2) \quad (2)$$

where E_T is the total energy of the system calculated with the same supercell. A positive E_b indicates that the defect pairs tend to bind to each other when both are present in the sample. The calculated bind energies E_b of several defect pairs within the LDA and LDA+U approaches are positive, as shown in Figure 2, indicating that the defects pairs are stable with respect to the isolated impurities in the host lattice. The large binding energy can be understood to form the defect complex.[15,43] The donor levels donate one or two electrons to one of the acceptors, forming the neutral and charge defect pairs, which results in a large Coulomb interation between donor and acceptor impurities (e.g., between Nb_{Ti}^{1+} and C_O^{2-}). As the electronegativity decreases from N to C, the Coulomb binding energy decreases.

To further determine the stable codoped configurations, we constructed several nearest-neighbor codoping systems and then calculated their total energies. Two O sites and three Ti sites are labeled with numbers 1−5, as shown in Figure 3. For Nb/C-, Nb/N-, and Ta/N-codoped TiO_2, the (1, 3) configurations have lower total energies than the (2, 3) configurations (the differences are 0.089, 0.043, and 0.049 eV, respectively). On contrary, for Ta/C-codoped TiO_2, the total energy of the (2, 3) configuration is 0.015 eV lower than that of the (1, 3) configuration. In 1:2 codoped case, the (5, 1, 3) configuration is 0.063 eV energetically favorable than the (4, 1, 3) configuration for Nb/C/Nb-codoped TiO_2, whereas the (4, 1, 3) configuration is favorable by 0.008 eV than the (5, 1, 3) configuration for Ta/C/Ta-codoped TiO_2. In succedent work, we only focus on the configurations of the lowest energy for 1:1 and 1:2 codoped systems. In every case, the geometrical optimization is always made and the convergence is assured when the forces on atoms are less than 0.05 eV/Å, based upon which the electronic structures are calculated.

In the Nb_{Ti} configuration, the internuclear distances to the coordinating oxygens are r_{Nb-O} = 1.982 Å (+1.4%) on the xy plane and r_{Nb-O} = 2.010 Å (+0.6%) along the z axis. The numbers in parentheses show the changes relative to the lattice parameters of the pure TiO_2 calculated by us. The extension of the chemical bonds can been rationalized in light of the ionic radius of the two, that is, r = 0.61 Å for Ti^{4+} and r = 0.64 Å for Nb^{5+}.[44] Experimental X-ray absorption spectroscopy reported previously suggests that the Nb atoms have the charge state of Nb^{5+} and are located in distorted octahedral sites.[45] However, the position of the Nb_{Ti} did not change remarkably from the position of the replaced Ti atom.[46] In the Ta_{Ti} case, the effect of Ta doping on the geometry is nearly identical to that of Nb doping, due to the large space in the TiO_6 octahedra. In the N_O configuration, the Ti−N bond lengths, 1.956 and 2.041 Å, are slightly longer than the original Ti−O ones, 1.954 and 1.997 Å, respectively. The structural changes for replacing an O with a C atom are more noticeable than ones for replacing an O with a N atom.

For the Nb/N- and Ta/N-codoped TiO_2, the lattice distortion is significantly moderated by the compensation between the opposite actions induced by codoping. The phenomenon is also reported in ref 47. The lattice distortion of Nb/C-codoped TiO_2 is larger than that of Nb/N-codoped TiO_2 due to NCP codoping with the −1 charge state. In the Nb/C/Nb-codoped configuration, the two Nb−C bonds have the same length (1.987 Å), which is slight longer than the original Ti−O bond. It is obvious that 1:2 CP codoping systems suffer less stress and strain. To further investigate the effect of doping on the structure stability, in the next section, the dopant formation energies are calculated under O-rich and Ti-rich conditions.

3.2. Formation Energy. In thermodynamic equilibrium, the concentration c of point defects is given by the expression $c = N_{site}N_{config}\exp(-E_f/kT)$.[48] Here, E_f is the defect formation energy, and a lower E_f means a higher defect concentration c, which directly determines the physical and chemical behavior of TiO_2. In other words, defects with lower formation energies are more likely to form. To explore the possibility and stability of doping and optimal growth conditions, the calculations of the dopant formation energies have been performed, according to the expression[14−17,49]

$$E_f = E_T(\text{doped}) - E_T(\text{undoped}) - n_{NM}\mu_{NM} - n_M\mu_M + n_O\mu_O + n_{Ti}\mu_{Ti} \quad (3)$$

where E_T(doped) and E_T(undoped) are the total energies of the codoping systems containing all the impurities, of the pure host supercell, respectively. μ_{NM} and μ_M are the chemical potentials of the nonmetal elements and metal elements, respectively; μ_O-(μ_{Ti}) is that of O(Ti). n_{NM} and n_M are the numbers of the host atoms substituted by nonmetal atoms and metal atoms, respectively. The formation energy depends on growth conditions, which may be varied from Ti- to O-rich. For TiO_2, μ_O and μ_{Ti} satisfy the following relationship: $2\mu_O + \mu_{Ti} = \mu(TiO_2)$. Here, gas O_2 and N_2, graphite, *hcp* bulk metal Ti, *bcc* bulk metal Nb, and *bcc* bulk metal Ta are used to determine the chemical potentials: $\mu_O = \mu(O_2)/2$, $\mu_N = \mu(N_2)/2$, $\mu_C = \mu(\text{graphite})/4$, $\mu_{Ti} = \mu_{Ti}^{metal}$, $\mu_{Ta} = \mu_{Ta}^{metal}$, and $\mu_{Nb} = \mu_{Nb}^{metal}$. To study the relation between the defect formation energies and the chemical potential of O, the

Table 1. Formation Energies E_f for Codoped TiO_2 (eV) under Ti-Rich or O-Rich Conditions within the LDA+U Approach. Δr is the Displacement of Nb(Ta) Atoms from the Position of an Original Ti Atom in the TiO_6 Octahedron

impurity	Ti-rich	O-rich	Δr
C	3.87	9.02	
N	0.03	5.18	
Nb/C	−0.03	−5.18	0.488
Nb/N	−4.00	−9.16	0.263
Nb/C/Nb	−3.56	−19.01	0.448/0.435
Ta/C	2.51	−2.64	0.331
Ta/N	−1.52	−6.67	0.265
Ta/C/Ta	1.79	−13.66	0.460/0.457

formation enthalpy $\Delta H_f[TiO_2]$ is expressed as $\Delta H_f[TiO_2] = \Delta\mu_{Ti} + \Delta\mu_O = (\mu_{Ti} - \mu_{Ti[bulk]}) + 2(\mu_O - \mu_{O[O_2]})$. According to our previous study,[49] $\Delta H_f[TiO_2] = -10.3$ eV; thus, -5.15 eV $\leq \Delta\mu_O \leq 0$. In other words, $\Delta\mu_O = 0$ eV indicates under extreme O-rich conditions and $\Delta\mu_O = -5.15$ eV indicates under extreme T-rich conditions.

The calculated formation energies for the substitutions of O by C are 9.02 and 3.87 eV under O-rich and Ti-rich conditions, respectively, which are larger than that of N-monodoped TiO_2 (5.18 and 0.03 eV). This indicates that C monodoping is relatively more difficult than N monodoping. Although N_O and C_O induce some acceptor levels in the band gap, the previous studies show that p-type doping remains difficult due to the low VBM and strong self-compensation.[13,15,43] For the Nb/N- and Ta/N-codoped TiO_2, the formation energies are about −9.16 and −6.67 eV under O-rich conditions, respectively, which are much less than that by doping with N alone. The reduced formation energies by codoping indicate that the concentration of the N impurity in the host lattice can be greatly enhanced in the presence of Nb or Ta doping. It suggests that TM/nonmetal codopings are facilitated by the electrostatic attraction of the two dopants with opposite charge states.[13] A similar phenomenon is also reported in ref 50.

The calculated formation energies of codoping are listed in Table 1. There are several features: (1) Under O-rich conditions, the formation energies of these codoped configurations are less than those under Ti-rich conditions. It shows that all these codoped systems are more likely to be formed under O-rich conditions. (2) All of the codoped TiO_2 with Nb have lower dopant formation energies than those of codoped TiO_2 with Ta, partly because of the larger radius of the Ta atom.[15,44] (3) Under O-rich conditions, the 1:2 CP codoped systems are more energetically favorable than 1:1 NCP codoped systems. It can be explained that the configurations codoped with another Nb (Ta) make the doping easier by symmetrizing and balancing the stress on the C atoms. As a result, Nb/C/Nb- and Ta/C/Ta-codoped systems can be formed easily under O-rich conditions. In principle, the codoping approach can overcome the p-type doping bottleneck, and it is easy to control the dopant concentration under different growth conditions.[13,15,50] Especially, the dopant formation energies of CP systems are lower than that of NCP systems, which indicates that the CP codoping greatly facilitates the enhancement of the concentration of p-type dopants in the host lattice.

3.3. Electronic Properties. To compare modifications in the electronic structure of different doped systems, the density of states (DOS) and the projected DOS (PDOS) are calculated. Our previous results show that the VB edge is mainly contributed by O 2p states, whereas the CB edge consists mainly of Ti 3d states.[51] For N-monodoped TiO_2, it is clear from Figure 4a that two isolated N 2p states are localized just 0.30 eV above the top of the VB of the host TiO_2 because N is less electronegative than O. The upshift of the VBM is only 0.04 eV without altering the CBM, and thus, the energy gap is about 2.89 eV. Therefore, it is reasonable to consider that the N-derived localized energy state above the top of the VB (as indicated in Figure 4a) cannot be expected to significantly influence the optical absorption property.[51] In addition, N doping creates a partially occupied impurity band in the band gap of the host TiO_2 due to deficient an electron on N 2p levels. It has been proved that the reduction of Ti^{4+} to Ti^{3+} occurs in N-doped TiO_2 due to the charge imbalance between O^{2-} ions and N^{3-} ions.[52] Figure 4b shows that three isolated C 2p states (two occupied and one empty) as deep acceptors appear in the band gap for C-monodoped TiO_2, with less mixing with that of O 2p, which gives rise to the large red shift in the absorption edge. In other words, the electrons in the VB can be excited to localized impurity states in the band gap and subsequently to the CB under visible-light irradiation. However, the empty C 2p states can act as traps for excited electrons, which can promote recombination rates of electron−hole pairs.[5]

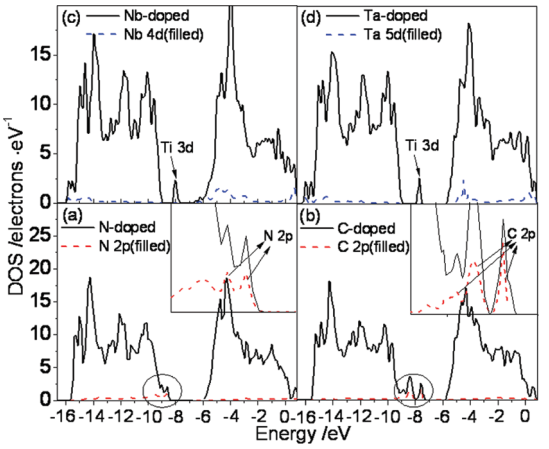

Figure 4. Total DOS and corresponding PDOS of the dopant in the TiO_2 lattice: (a) N-doped TiO_2, (b) C-doped TiO_2, (c) Nb-doped TiO_2, and (d) Ta-doped TiO_2. Here, we only showed spin-up DOS. The insets in (a) and (b) show the enlarged two N 2p states and three C 2p states, which are indicated by dashed arrows.

The DOS of Nb-monodoped TiO_2 calculated with standard DFT show that no new states are found in the fundamental band gap. Instead, the Nb 4d states are distributed throughout the CB and the excess charge occupies the bottom of the CB. The results disagree with experimental PES data that show a defect state in the band gap well separated from the CB, with a height proportional to the Nb concentration.[53] Our calculated DOS with the LDA+U approach are in good agreement with experiment, showing a narrow peak in the band gap (1.4 eV above the top of the VB), as shown in Figure 4c. Figure 4d shows that the DOS of Ta-monodoped TiO_2 calculated with the LDA+U approach is nearly identical to that of Nb-monodoped TiO_2, a gap state 1.5 eV above the top of the VB. Morgan et al. presented the projection of the charge associated with the gap state, which shows occupation of the Ti $3d_{xy}$ on one of the nearest-neighbor cation sites, with no contribution from the Ta 5d state.[54]

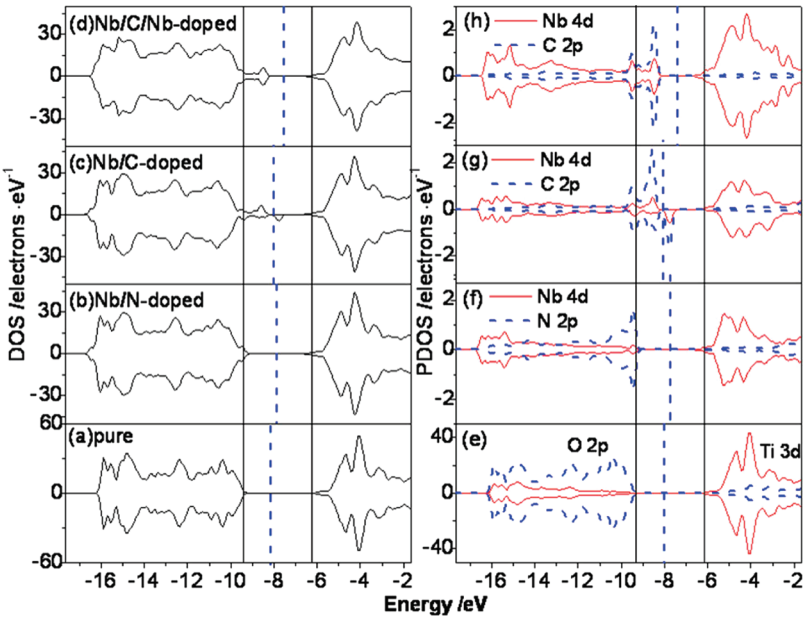

Figure 5. DOS (left) for (a) pure TiO_2, (b) Nb/N-doped TiO_2, (c) Nb/C-doped TiO_2, and (d) Nb/C/Nb-doped TiO_2. The corresponding PDOS are shown on the right in (e)−(h).

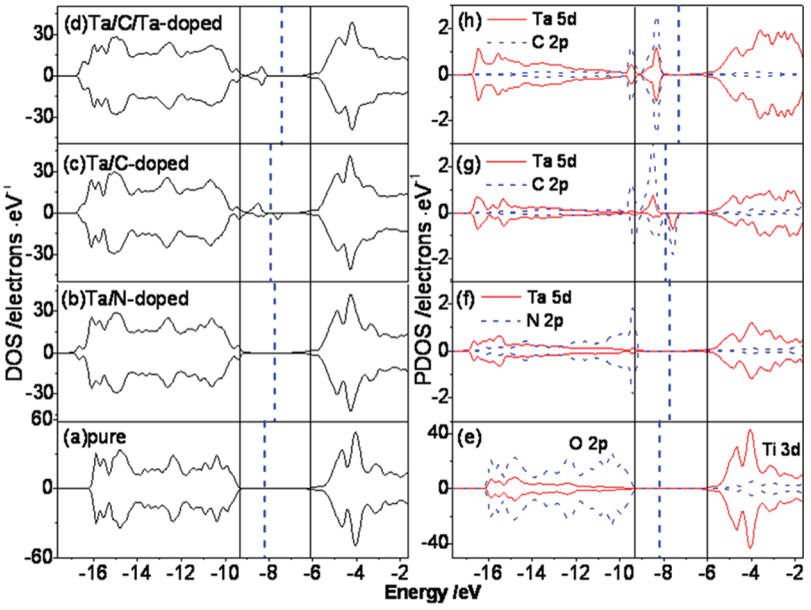

Figure 6. DOS (left) for (a) pure TiO_2, (b) Ta/N-doped TiO_2, (c) Ta/C-doped TiO_2, and (d) Ta/C/Ta-doped TiO_2. The corresponding PDOS are shown on the right in (e)−(h).

For Nb/N- and Ta/N-codoped TiO_2, no isolated energy states appear in the band gap, as shown in Figures 5b and 6b. In other words, the Nb(or Ta)-derived impurity bands vanish from the band gap. The Fermi level lies above the N 2p states, suggesting its full occupation and rendering these systems less likely to form electron−hole recombination centers. However, the energy gap reductions for Nb/N- and Ta/N-codoped TiO_2 are 0.1 and 0.3 eV (corresponding to the extension of the absorption edge about 12.5 and 40.1 nm), respectively, far less for the requirement of red shifting the absorption edge into the optimal visible-light region. Although no recombination center has been formed, the Nb/N- and Ta/N-codoped systems have a limited ability in visible-light photocatalytic activity.

In Nb/C (Ta/C) codoping configurations, an O atom and a Ti atom are replaced by a C atom and a Nb (Ta) atom, respectively. It is well known that C has two fewer valence electrons than O, and Nb (Ta) has one more valence electron than Ti. Therefore, both 1:1 Nb/C and Ta/C codopings are noncompensated. Two distinct features are observed. First, it is clear in Figure 5g that hybridized C 2p and Nb 4d states are located in the band gap, leaving the CBM almost unchanged and thus reducing the energy gap by 1.50 eV. Second, the analysis of the PDOS indicates that

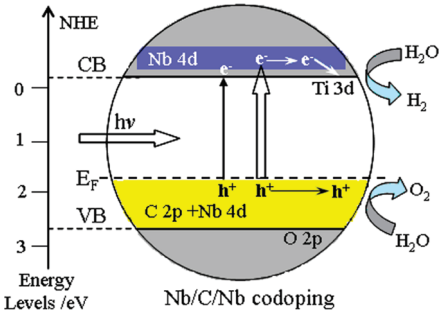

Figure 7. Schematic illustration of the band structure of Nb/C/Nb-codoped anatase TiO_2.

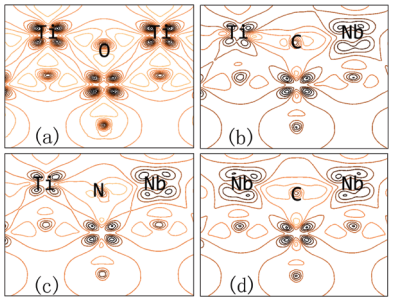

Figure 8. Difference between charge density and the superposition of atomic densities for the (1 0 0) plane: (a) pure TiO_2, (b) Nb/C-doped TiO_2, (c) Nb/N-doped TiO_2, (d) Nb/C/Nb-doped TiO_2.

the codoping brings about more distortion of anatase TiO_2. The distorted crystal field splits the energy band of the hybridized C 2p and Nb 4d, and the Fermi level locates between the spin-up and spin-down states. So is Ta/C-codoped TiO_2. The partially occupied impurity states can easily trap the carriers and lead to the reduction in carrier mobility and conversion efficiency,[5,51] which is a drawback for the application of monodoped and NCP codoped TiO_2 in the photoelectrochemical conversion of solar energy. Thus, although these NCP codoped systems have a significant reduction of the phototransition energy, they are not so suitable for enhancing the photocatalytic activity in the visible-light region. This view does not conflict with that of ref 47. Pan and co-workers think that NCP CrO codoping improves the carrier mobility of GaN because the effect of local trapping is eliminated relative to that of Cr monodoping.

To eliminate the partially occupied impurity states, the 1:2 configurations (i.e., Nb/C/Nb and Ta/C/Ta codoping) are constructed and then their DOS and PDOS are calculated. Obviously, hybridized states composed of C 2p orbitals and Nb 4d or Ta 5d orbitals are formed. In particular, the hybridized states locate mainly at the VB edge, while leaving the CBM almost unchanged (only 0.1 eV lower than that of pure TiO_2), thus reducing the energy gap by about 1.17 eV for Nb/C/Nb-codoped TiO_2 and 1.25 eV for Ta/C/Ta-codoped TiO_2, respectively, as shown in Figures 5h and 6h. As C acts as a double acceptor and Nb (Ta) acts as a single donor, codoping with one acceptor and two donors, respectively, can compensate for the charges of the impurities from each other. In other words, two electrons move from the partially occupied Nb 4d (Ta 5d) orbitals to the partially occupied C 2p orbitals. The Fermi level lies above the hybridized states, and full occupied C 2p states appear. As discussed above, both 1:2 Nb/C/Nb and Ta/C/Ta codopings are compensated. For Nb/C/Nb-codoped TiO_2, Nb 4d states may be responsible for the lowering of the energy levels of C 2p states, bringing the C 2p states much closer to the VB and, therefore, enhancing the mixing of C 2p and O 2p states in the VB. In this case, continuum states above the VB edge are formed rather than isolated states, which is favorable toward enhancing the lifetimes of photoexcited carriers.[55] It is similar to the phenomenon appearing in N/H-codoped TiO_2.[56] For the Ta/C/Ta-codoped TiO_2, Ta 5d states contribute less in the lowering of the C 2p states and the configuration is less balanced both geometrically and electronically, so the isolated states are formed. However, the CP systems keep the semiconductor character, which subsequently promotes the separation of electron−hole pairs excited under visible-light irradiation. These results indicate that the 1:2 CP systems guarantee a significant photocatalytic activity in the visible-light region by narrowing the energy gap to nearly 2 eV and suppress the recombination of electron−hole pairs. Figure 7 is a schematic illustration of the band structure of Nb/C/Nb-codoped anatase TiO_2.

For a further understanding of the transfer mechanism of the electrons, we plotted the charge density differences of codoped and pure TiO_2. Figure 8c shows that, for the Nb/N-codoped situation, electrons move from Nb 4d orbitals to N 2p orbitals, and shallow states appear. For Nb/C-codoped TiO_2, the electrons around Nb atom are so nonlocalized that partially occupied C 2p states appear, as shown in Figure 8b. What's more, we have confirmed that an electric dipole between Nb and C atoms is more than one between Nb and N. Figure 8d shows that electrons from both sides of Nb atoms move to C atoms and fill the C 2p states for the Nb/C/Nb-codoped system. In fact, Ta/C/Ta codoping has similar charge density differences to Nb/C/Nb codoping. The Nb−C bond with a short distance indicates that two NbO_5N octahedrons are strongly distorted, in which Nb^{5+} ions are displaced by 0.448 and 0.435 Å from the position of an original Ti atom in the TiO_6 octahedron, as shown in Table 1. On the basis of the displacement of two Nb^{5+} ions, there are two dipole moments of 8.747 and 8.493 D (D = debye) generated inside the octahedral coordination. The dipole moment causes an internal local polarization field that promotes the separation of photoexcited holes and electrons, which plays an important role in photocatalysis.[57−59]

4. CONCLUSIONS

We have proposed the use of the codoping concept to improve the material property limitation that must be addressed before it can be considered for photoelectrochemical water splitting. On the basis of the codoping TiO_2 with Nb (Ta) and C, the following conclusions are considered: (1) Nonmetal−metal defect pairs in the host TiO_2 tend to bind to each other, and the formation energy of an anion doping is greatly reduced by codoping with the cation, including 1:1 and 1:2 codoped TiO_2 systems, which facilitate the enhancement of the concentration of p-type dopants. (2) The hybridized states of Nb 4d (Ta 5d) and C 2p orbitals above the top of the VB for these codopings should be responsible for the red shift of the optical absorption edge. (3) Codopings almost do not change the CBM and thus do not affect the reducibility of electrons in the conduction band. (4) The CP codoping can eliminate the local trapping, which improves the carrier mobility. It is demonstrated theoretically that Nb/C/Nb- and Ta/C/Ta-codopings can be candidates for

considerable enhancement of the photocatalytic activity of anatase TiO_2 in the visible-light region.

AUTHOR INFORMATION

Corresponding Author

*E-mail: zhuyf@mail.tsinghua.edu.cn. Tel: (+86)10-6278-3586. Fax: (+86)10-6278-7601.

ACKNOWLEDGMENT

This work was supported by the National Natural Science Foundation of China (20925725 and 50972070), the National Postdoctoral Science Foundation of China (20100480254), and the National Basic Research Program of China (2007CB613303). The authors gratefully acknowledge Professor Huijun Liu for valuable discussions on this topic.

REFERENCES

(1) Linsebigler, A. L.; Lu, G.; Yates, J. T. *Chem. Rev.* **1995**, *95*, 735.
(2) Hadjiivanov, K.; Klissurski, D. G. *Chem. Soc. Rev.* **1996**, *25*, 61.
(3) Wang, P.; Zakeeruddin, S. M.; Moser, J. E.; Nazeeruddin, M. K.; Sekiguchi, T.; Grätzel, M. *Nat. Mater.* **2003**, *2*, 402.
(4) Asahi, R.; Morikawa, T.; Ohwaki, T.; Aoki, K.; Taga, Y. *Science* **2001**, *293*, 269.
(5) Irie, H.; Watanabe, Y.; Hashimoto, K. *J. Phys. Chem. B* **2003**, *107*, 5483.
(6) Valentin, C. D.; Pacchioni, G.; Selloni, A. *Phys. Rev. B* **2004**, *70*, 085116.
(7) Yang, K. S.; Dai, Y.; Huang, B. B. *J. Phys. Chem. C* **2007**, *111*, 12086.
(8) Yang, K. S.; Dai, Y.; Huang, B. B.; Han, S. H. *J. Phys. Chem. B* **2006**, *110*, 24011.
(9) Finazzi, E.; Valentin, C. D.; Selloni, A.; Pacchioni, G. *J. Phys. Chem. C* **2007**, *111*, 9275.
(10) Khan, S. U. M.; Al-Shahry, M.; Ingler, W. B. *Science* **2002**, *297*, 2243.
(11) Valentin, C. D.; Pacchioni, G.; Selloni, A. *Chem. Mater.* **2005**, *17*, 6656.
(12) Yang, K. S.; Dai, Y.; Huang, B. B. *Phys. Rev. B* **2007**, *76*, 195201.
(13) Wei, S. H. *Comput. Mater. Sci.* **2004**, *30*, 337.
(14) Yan, Y. F.; Wei, S. H. *Phys. Status Solidi B* **2008**, *245*, 641.
(15) Gai, Y. Q.; Li, J. B.; Li, S. S.; Xia, J. B.; Wei, S. H. *Phys. Rev. Lett.* **2009**, *102*, 036402.
(16) Zhao, Z. Y.; Liu, Q. J. *Catal. Lett.* **2008**, *124*, 111.
(17) Yin, W. J.; Tang, H. W.; Wei, S. H.; Al-Jassim, M. M.; Turner, J.; Yan, Y. F. *Phys. Rev. B* **2010**, *82*, 045106.
(18) Gu, D. E.; Yang, B. C.; Hu, Y. D. *Catal. Commun.* **2008**, *9*, 1472.
(19) Liu, J. W.; Han, R.; Zhao, Y.; Wang, H. T.; Lu, W. J.; Yu, T. F.; Zhang, Y. X. *J. Phys. Chem. C* **2011**, *115*, 4507.
(20) Zhu, W.; Qiu, X.; Iancu, V.; Chen, X.; Pan, H.; Wang, W.; Dimitrijevic, N. M.; Rajh, T.; Meyer, H. M.; Paranthaman, M. P.; Stocks, G. M.; Weitering, H. H.; Gu, B.; Eres, G.; Zhang, Z. *Phys. Rev. Lett.* **2009**, *103*, 226401.
(21) Huang, Y.; Ho, W. K.; Ai, Z. H.; Song, X.; Zhang, L. Z.; Lee, S. C. *Appl. Catal., B* **2009**, *89*, 398.
(22) Osorio-Guillén, J.; Lany, S.; Zunger, A. *Phys. Rev. Lett.* **2008**, *100*, 036601.
(23) Lany, S.; Zunger, A. *Phys. Rev. B* **2005**, *72*, 035215.
(24) Soler, J. M.; Artacho, E.; Gale, J. D.; García, A.; Junquera, J.; Ordejón, P.; Sánchez-Portal, D. *J. Phys.: Condens. Matter* **2002**, *11*, 2745.
(25) Troullier, N.; Martins, J. L. *Phys. Rev. B* **1991**, *43*, 1993.
(26) Monkhorst, H. J.; Pack, J. D. *Phys. Rev. B* **1976**, *13*, 5188.
(27) Kohn, W.; Sham, L. J. *Phys. Rev.* **1965**, *140*, A1133.
(28) Perdew, J. P.; Burke, K.; Ernzerhof, M. *Phys. Rev. Lett.* **1996**, *77*, 3865.
(29) Kiliç, Ç.; Zunger, A. *Phys. Rev. Lett.* **2002**, *88*, 095501.
(30) Walsh, A.; DaSilva, J. L. F.; Wei, S. H. *Phys. Rev. Lett.* **2008**, *100*, 256401.
(31) Lathiotakis, N. N.; Andriotis, A. N.; Menon, M. *Phys. Rev. B* **2008**, *78*, 193311.
(32) Park, S. G.; Magyari-Köpe, B.; Nishi, Y. *Phys. Rev. B* **2010**, *82*, 115109.
(33) Sheetz, R. M.; Ponomareva, I.; Richter, E.; Andriotis, A. N.; Menon, M. *Phys. Rev. B* **2009**, *80*, 195314.
(34) Ma, X. G.; Lu, B.; Li, D.; Shi, R.; Pan, C. S.; Zhu, Y. F. *J. Phys. Chem. C* **2011**, *115*, 4680.
(35) Henrich, V. E.; Dresselhaus, G.; Zeiger, H. J. *Phys. Rev. Lett.* **1976**, *36*, 1335.
(36) Göpel, W.; Anderson, A.; Frankel, D.; Jaehnig, M.; Phillips, K.; Schäfer, J. A.; Rocker, G. *Surf. Sci.* **1984**, *139*, 333.
(37) Morgan, B. J.; Watson, G. W. *Surf. Sci.* **2007**, *601*, 5034.
(38) Lany, S.; Zunger, A. *Phys. Rev. B* **2009**, *80*, 085202.
(39) Mori-Sánchez, P.; Cohen, A. J.; Yang, W. *Phys. Rev. Lett.* **2008**, *100*, 146401.
(40) Morgan, B. J.; Watson, G. W. *Phys. Rev. B* **2009**, *80*, 233102.
(41) Burdett, J. K.; Hughbanks, T.; Miller, G. J.; Richardson, J. W.; Smith, J. V. *J. Am. Chem. Soc.* **1987**, *109*, 3639.
(42) Lazzeri, M.; Vittadini, A.; Selloni, A. *Phys. Rev. B* **2001**, *63*, 155409.
(43) Wang, D.; Zou, Y. H.; Wen, S. C.; Fan, D. Y. *Appl. Phys. Lett.* **2009**, *95*, 012106.
(44) Shannon, R. D. *Acta Crystallogr., Sect. A* **1976**, *32*, 751.
(45) Sacerdoti, M.; Dalconi, M. C.; Carotta, M. C.; Cavicchi, B.; Ferroni, M.; Colonna, S.; Di Vona, M. L. *J. Solid State Chem.* **2004**, *177*, 1781.
(46) Liu, X. D.; Jiang, E. Y.; Li, Z. Q.; Song, Q. G. *Appl. Phys. Lett.* **2008**, *92*, 252104.
(47) Pan, H.; Gu, B. H.; Eres, G.; Zhang, Z. Y. *J. Chem. Phys.* **2010**, *132*, 104501.
(48) Van de Walle, C. G.; Neugebauer, J. *J. Appl. Phys.* **2004**, *95*, 3851.
(49) Ma, X. G.; Jiang, J. J.; Liang, P. *Acta Phys. Sin.* **2008**, *57*, 3120.
(50) Ahn, K.-S.; Yan, Y. F.; Shet, S.; Deutsch, T.; Turner, J.; Al-Jassim, M. *Appl. Phys. Lett.* **2007**, *91*, 231909.
(51) Ma, X. G.; Miao, L.; Bie, S. W.; Jiang, J. J. *Solid State Commun.* **2010**, *150*, 689.
(52) Nakano, Y.; Morikawa, T.; Ohwaki, T.; Taga, Y. *Appl. Phys. Lett.* **2005**, *86*, 132104.
(53) Morris, D.; Dou, Y.; Rebane, J.; Mitchell, C. E. J.; Egdell, R. G.; Law, D. S. L.; Vittadini, A.; Casarin, M. *Phys. Rev. B* **2000**, *61*, 13445.
(54) Morgan, B. J.; Scanlon, D. O.; Watson, G. W. *J. Mater. Chem.* **2009**, *19*, 5175.
(55) Tang, J.; Ye, J. *Chem. Phys. Lett.* **2005**, *410*, 104.
(56) Mi, L.; Xu, P.; Shen, H.; Wang, P. N. *Appl. Phys. Lett.* **2007**, *90*, 171909.
(57) Sato, J.; Kobayashi, H.; Inoue, Y. *J. Phys. Chem. B* **2003**, *107*, 7970.
(58) Long, M.; Cai, W.; Wang, Z.; Liu, G. *Chem. Phys. Lett.* **2006**, *420*, 71.
(59) Inoue, Y. *Energy Environ. Sci.* **2009**, *2*, 364.